DOI: 10.13009/EUCASS2019-756

Effect of microstructure and temperature on the impact toughness of forged Ti-6Al-4V

M.J. Viscasillas[a], N.M. Piris[b], E.M. Andrés[c], M.V. Aguirre[d], J.M. Antoranz[e], J.A. Heredero[f]
Department of Aerospace Materials and Production, Universidad Politécnica de Madrid (UPM)
Pza. Del Cardenal Cisneros 3, 28040 (Madrid)
a – mj.viscasillas@upm.es, b – nuria.mpiris@upm.es, c – eva.andres.lopez@upm.es,
d – mariavega.aguirre@upm.es, e – juanmanuel.antoranz@upm.es, f – joseantonio.heredero@upm.es

Abstract

Titanium alloys are widely used in the aerospace industry for structural and engine components. One of the mechanical properties that are required in this field is the impact toughness. In titanium alloys, this property is affected by the microstructure and the working temperature. In this study, an α+β annealing and a β annealing heat treatments of forged Ti-6Al-4V are tested at different temperatures using a Charpy impact testing machine. Fracture mechanisms are studied both macroscopically and microscopically to relate their behavior with the temperature. Mixture brittle-ductile fracture mechanisms are observed in the scanning electron microscope.

1. Introduction

Titanium is a light metal two times heavier than aluminium and with almost half of the weight of iron or nickel. Due to its low weight, the specific strength of titanium alloys makes them usable in structural parts, especially when the excess of weight can be a problem. In addition, its excellent corrosion behaviour in almost all the environments makes more suitable their use in more demanding applications. Another important factor is the capacity to maintain good mechanical properties at a certain temperatures, taking advantage from the aluminium alloys and carbon fibre composites. At higher temperatures than 500ºC, some titanium alloys can be applied but their mechanical properties start to drop and can be affected by oxidation processes [1].

In this study, Ti-6Al-4V alloy was used to analyse the impact toughness behaviour under different conditions. Ti-6Al-4V alloy is classified as α+β titanium alloy, where aluminium stabilises the α-phase having a hexagonal close packed lattice and the vanadium stabilises the β body centred cubic phase. Thanks to the appearance of this two different phases, the behaviour of the material can be modified by the application of different heat treatments to obtain different microstructures. The most common microstructures of α+β titanium alloys are the duplex microstructure where a mixture of α-grains and laminar α surrounded by β-phase coexist, the lamellar or Widmanstätten α structure with β-phase around the platelets and, at last, the martensitic microstructure by applying a fast cool down.

Despite the fact that the trends in the new development of aerospace vehicles are more focused on composite materials, especially polymer matrix composites, Ti-6Al-4V alloy is still widely used in different parts of the structure and the gas turbine. Some examples of the structural application of this alloy in the aerospace industry are airframes, seat rails, windows frames, landing gear beams, etc. Referring to the engine applications, there are a lot of components from the fan like blades, disks, casings, and also in the first stages of the compressor in the form of casings, stators, manifolds, etc. Moreover, in the military aircraft industry titanium alloys have more importance than commercial aircrafts due to the higher requirements of these aircrafts [1] [2] [3].

One important factor that has to be taken into account is that for the aerospace industry, the safety is a major designing criterion and it is preferably that the materials used are forged. Castings are not used for structural parts and despite new manufacturing processes like additive layer manufacturing are being developed, there are still not real application in the aerospace industry due to their lower properties compared to the forged materials.

DOI: 10.13009/EUCASS2019-756

Impact toughness is the total energy that the material can absorb from an impact until its fracture. This is an important property when designing structural parts and some other critical pieces to avoid catastrophic accidents. As it has been mentioned before, the main applications of this alloy are structural parts and the first steps of the gas turbines because its maximum working temperature is around 300ºC. Although toughness is an important property limiting the possible applications, there are no exhaustive studies analysing the influence of the different possible microstructures on the optimization of the toughness for the mentioned applications. The characterisation of the impact toughness and the fracture mechanisms, both microscopic and macroscopic, from two different heat treatments, the (α+β)-annealing and the β-annealing, are studied in this work.

2. Material and preparation of the samples

In this work, all the test samples were obtained from a 20mm thickness plate of Ti-6Al-4V alloy. Its starting condition was the mill annealing and different heat treatments were applied from this point. The chemical composition of the alloy and the conditions of the heat treatments given are shown in **Table 1** and **Table 2** respectively. The conditions chosen to study the impact toughness are the (α+β)-annealing to obtain a duplex microstructure and the β-annealing to obtain α lamellar microstructure. Solution and aging treatments will be studied in future works.

Table 1: Chemical composition of Ti-6Al-4V alloy (wt. %)

Al	**V**	**Fe**	**C**	**N**	**H**	**O**	**Ti**
6.3	4.0	0.18	0.01	0.01	0.004	0.10	Bal.

Table 2: Heat treatment conditions

Heat Treatment	**T_1 (ºC)**	**t_1 (min)**	**T_2 (ºC)**	**t_2 (h)**
α+β Annealing	940	60	675	4
β Annealing	1025	25	720	2

All the cool downs were done inside the furnace.

The Charpy V-notch sample dimensions are described in **Figure 2**. As the Charpy sample is thinner than the thickness of the plate, the plate was machined till the thickness got 11mm removing material to obtain the Charpy samples from the central part of the thickness of the plate. After that, the heat treatments were applied using a vacuum furnace to avoid the apparition of α case due to the diffusion of oxygen inside the plate at high temperatures. Once the heat treatments were finished, the 11mm thickness plates were machined to their final thickness, and right after the samples were cut in the transversal direction to get the square based prisms. For this work, the samples studied were L-T, where the samples were parallel to the longitudinal direction of the plate, and the notch was machined in the transverse direction

DOI: 10.13009/EUCASS2019-756

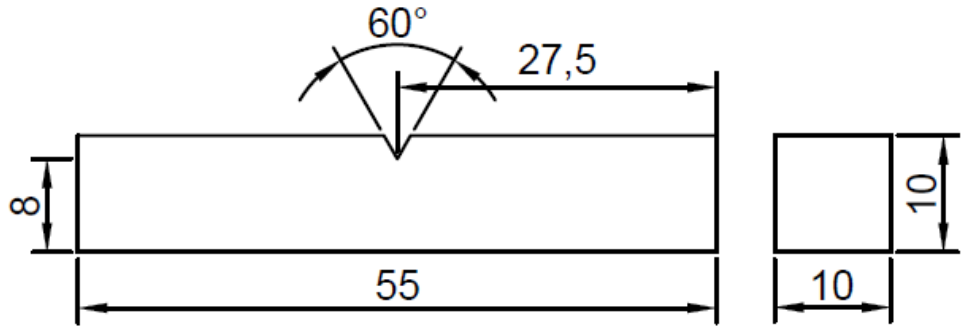

Figure 2. Schematic of the Charpy V-notch impact toughness sample. All the dimensions are in mm.

3. Experimental procedure

3.1 Impact toughness test

The impact toughness tests were carried on a 150J Charpy impact toughness pendulous with an analogical scale to measure the energy following the ASTM E23 standard [4]. Due to the short sensitivity of the measurements, a procedure of digital imaging was developed to improve the resolution of the results. The objective was to take a high resolution photograph of the scale to be able to measure the accurate point of the scale with ImageJ® software. With this system, the resolution in the energy measurements was improved from 2.5J to 0.1J. The energy units used in the scale were kg·m so to convert them in Jules, it has been used the value of gravity of 9.801m·s^{-2}.

For low temperature and high temperature tests, a Charpy V-notch sample was machined to be able to introduce a thermocouple inside the sample to control the temperature and some procedure simulations were done. For this kind of test, the low thermal conductivity of the titanium alloys made the procedure easier, due to the temperature of the sample remained constant for the enough time to do the tests. The cooling process for the -25ºC tests was done by introducing the samples inside an alcohol-filled recipient and after that introducing the entire recipient in a freezer. The samples where maintained inside the freezer until the temperature was fully stabilized in -25ºC. For the high temperature tests, the procedure was similar. A furnace was placed next to the Charpy impact toughness pendulous and the samples were introduced in the furnace. After several trials with the thermocouple sample, it was decided to raise the furnace temperature 5ºC for the 200ºC tests and 10ºC for the 400ºC. At higher temperatures, the cooling inertia was higher than at lower temperatures, but with this procedure, all the samples were done successfully in the desired temperature with a temperature variation of ±2ºC from the target temperature.

3.2. Fracture analysis

The measurement of the percent shear fracture was carried on following the ASTM E23 advices using the digital image analysis system. Once the impact toughness tests were done, the fractured surfaces of the samples were photographed in a Leica MZ8 macroscope with a Leica IC80 HD camera.

The graphical process of how this property was calculated is on **Figure 3**. Once the photograph was taken, using the GNU software GIMP2®, a transparent extra layer was added to the image to be able to paint over it and mark in yellow the effective fracture of the sample. After completing this, a different transparent layer was created over the image to repeat the process and identify the brittle plain fracture zone of the centre of the sample. The next step is to use ImageJ® software to calculate the total area of the sample with the first yellow marked image and the area of the brittle fracture zone delimited in the previous step. Calculating the difference of the percentages from this two sections is the percent of brittle fracture surface. The proportion of shear fracture surface is the remaining percentage till reach 100%.

DOI: 10.13009/EUCASS2019-756

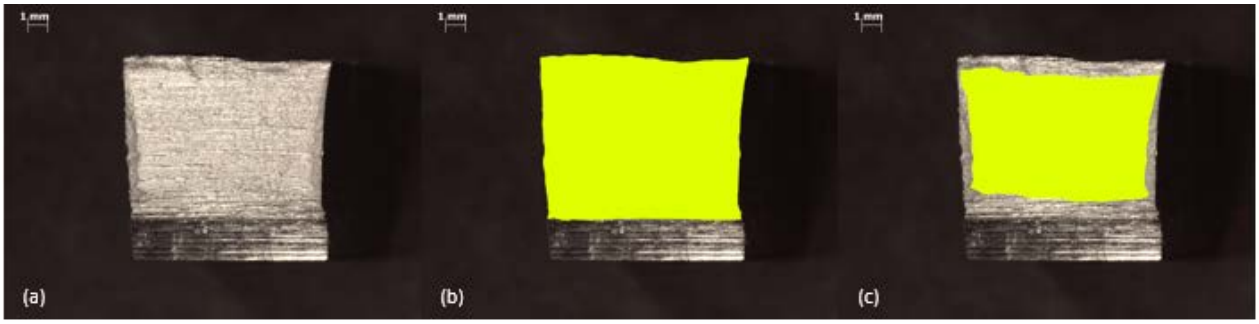

Figure 3. Steps for calculating the proportion of shear fracture surface. (a) Original image, (b) detection of the total surface of the sample, (c) Identification of the plain brittle fracture surface.

The micrographic fracture mechanisms of the samples were observed using a Hitachi S3400N scanning electron microscope. Samples were analysed from the notch to the impact face to check if there were differences along the propagation of the fracture. The photographs of each section were taken at the same set of magnifications to be able to do a direct comparison between different samples.

4. Results

The results have been grouped in four different sections, starting with the microstructures obtained by the application of the heat treatments, the values of the impact toughness and a comparison between other publications of other authors, the proportion of shear fracture surface and finally the fracture analysis.

4.1. Microstructures

When the heat treatments where done in the vacuum furnace, a small sample of the alloy was introduced with the plates to be able to study the resultant microstructure after the heat treatment. The resulting images taken from the optical microscope of both heat treatments are in **Figure 4**. On the left part is the (α+β)-annealing and on the right is the β-annealing microstructures.

The (α+β)-annealing was done at around 50-60ºC below the full β-phase transformation temperature, and for that reason there was a high quantity of alpha phase grains. In addition, as the soaking time inside the furnace of the samples was not too high, the preliminary morphology of the microstructure was not recrystallized so there are some reminders in the microstructure of the forging process. The darker parts of the image are a mixture of fine α-plates surrounded by β-phase. This composition of primary α-grains and laminar α surrounded by β-phase areas is defined as the duplex microstructure.
In the β-annealing heat treatment the temperature applied was just 25-30ºC above β-transus and the soaking time was short to minimize the worsening of the properties by obtaining big coarse grains. In **Figure 4 (b)**, the Widmanstätten structure is observed. The α-platelets surrounded by β-phase grow inside the old β-phase grains, having α-phase needles on the previous β-grain borders.

4.2. Impact toughness

Impact energy values of the different heat treatments and at different temperatures are given in **Figure 5**. The values shown are the mean of obtained of each temperature. The ASTM E23 standard says that if the impact energy obtained from the test exceeds the 80% of the pendulous capacity it must be reflected. For the 400ºC, all of the (α+β)-annealing samples exceeded that 80% of the total energy. The samples broke after the impact, so the values can be accepted. When giving the numerical values, the energy is expressed divided by surface to make easier the comparison between these results and previous works published by other authors.

DOI: 10.13009/EUCASS2019-756

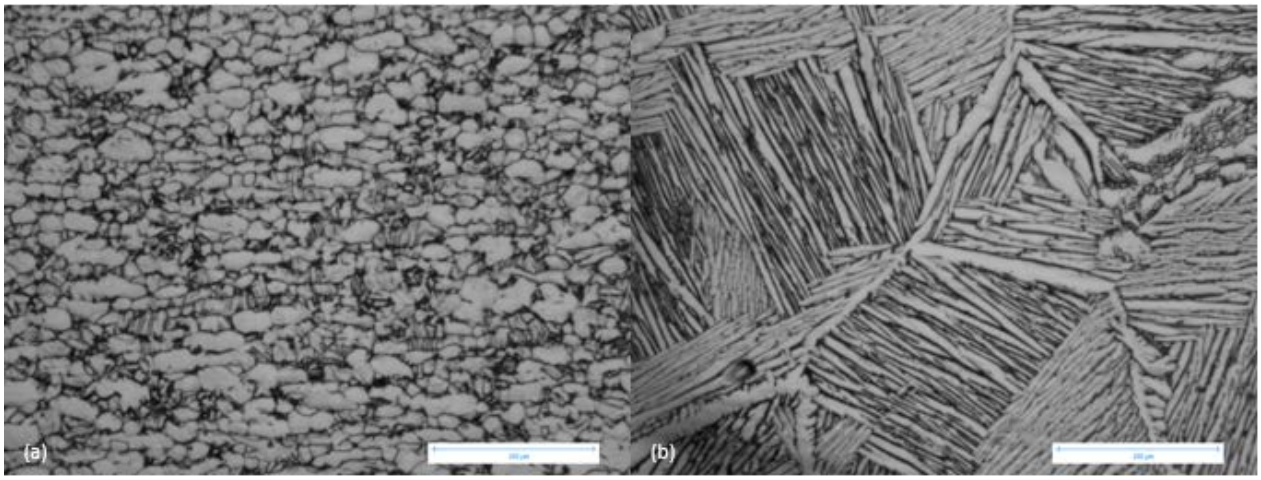

Figure 4. (a) Duplex microstructure of the (α+β)-annealing and (b) lamellar microstructure of the β-annealing.

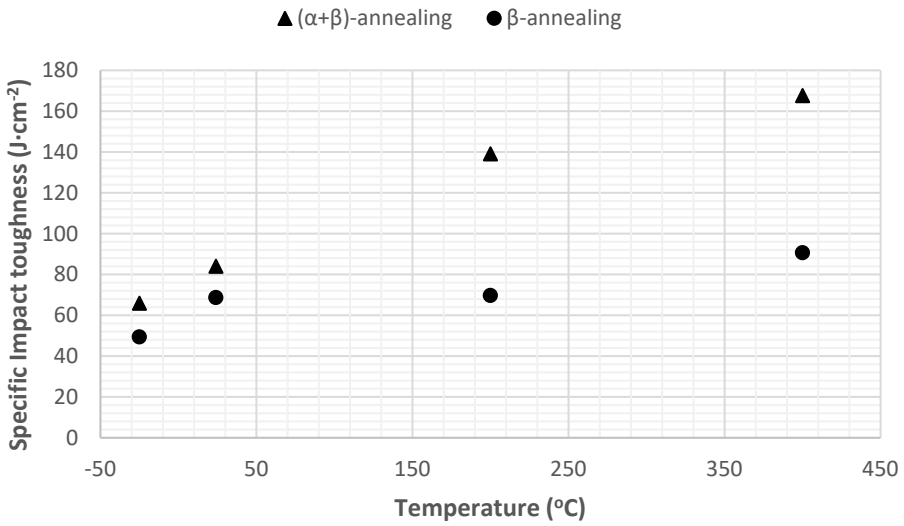

Figure 5. Impact toughness energies per surface versus temperature.

In the **Table 3** some of the results published by other authors are listed to be able to compare the data obtained in this study. Some of the studies are not done with standardized samples, so there are some differences in the total values. The impact toughness values have been referenced by the section to obtain comparable magnitudes. There are data from different manufacturing technologies, such as direct melting laser sintering manufacturing [5], forging processes [6] [8] and different welding techniques [7].

The most representative data to compare the results obtained is [6], due to the temperature testing is similar and it allows to observe the trends in the increasing on the impact toughness while increasing the temperature. There are differences in the magnitudes of the impact toughness, but the microstructural conditions were not the same. In this study, the duplex microstructure had lowlier cool down rates so the amount of α-equiaxed grains is bigger than the other study. This increase in equiaxed α-grains proportion affect diminishing the amount of laminar-α with β-phase surroundings areas, changing the behaviour of the alloy.

At lower temperatures, the material showed less energy absorption capacity than at higher temperatures, but the results obtained got higher values than the published by [6]. Comparing the sensitivity of the absorption energy rate with temperature, it is less sensitive because the slope is more horizontal than in [6]. This is observed in the difference between the impact energies of 200ºC and 400-500ºC. At 200ºC, the difference in the impact toughness energies is about 20%, but when comparing the estimation curve to reach 500ºC, the studied material would have 198J·cm^{-2} while the value in [6] is 283J·cm^{-2}. This difference can be influenced by the exceeding of the 80% energy capacity of the testing machine, but further studies will be done to understand it.

DOI: 10.13009/EUCASS2019-756

Table 3: Charpy impact toughness values from different sources

T (ºC)	Lamellar microstructure Impact toughness (J/cm²)	Duplex microstructure impact toughness (J/cm²)	Reference
-63	--	38	[6]
-25	49	65	
RT	68	84	
RT	--	36	[7]
RT	--	48	[6]
RT	--	24	[8]
200	--	112	[6]
200	69	139	
205	--	70	[8]
400	90	167	
500	--	283	[6]

Changing the attention to the β-annealing, the impact toughness was worse than the (α+β)-annealing but it had less temperature sensitivity during the tests. As it can be seen in the **Figure 5**, the slope of the trending line with the temperature is smaller than the trending slope of the (α+β)-annealing.

4.3. Proportion of shear fracture surface

It has been only possible to measure the results of the proportion of shear fracture surface from the (α+β)-annealing due to in the β-annealing heat treatment, the macroscopic fracture did not show this kind of behaviour of shear in the borders and plain brittle fracture in the inside. The numerical results are shown in **Figure 6**, and they confirm that at lower temperatures, there is less capacity of deformation than at higher temperatures. At -25ºC and room temperature, the proportion of shear fracture surface is almost similar, being at room temperature just 2% higher. When increasing the temperature, at 200ºC the proportion of shear fracture is higher, almost fifty percent more than at room temperature, and at 400ºC it is not possible to measure this proportion due to the macrostructure of the fracture.

This data is in correlation with the numerical values of the impact toughness tests. When increasing the temperature, the material impact toughness increases and it has more capacity to transform that absorbed energy into plastic deformation.

DOI: 10.13009/EUCASS2019-756

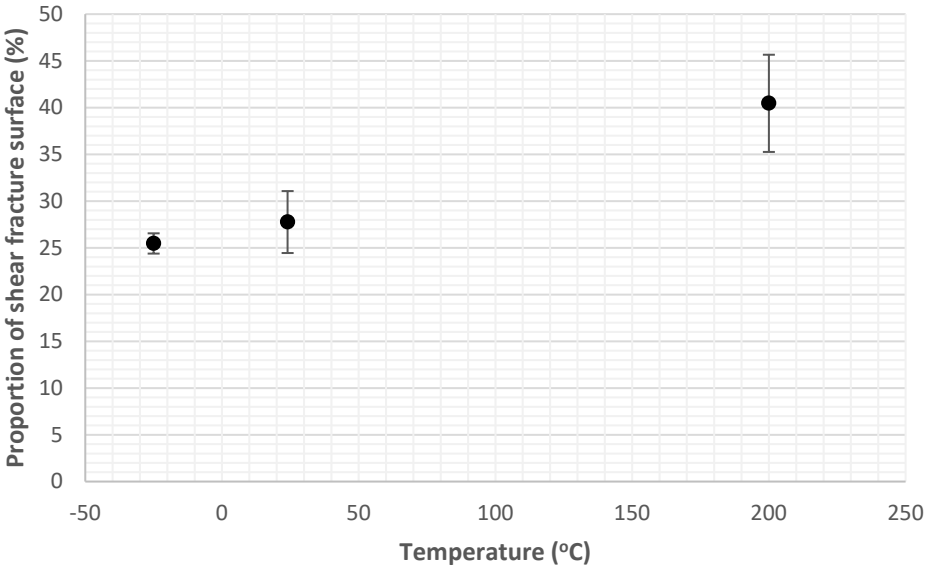

Figure 6. Proportion of shear fracture surface versus temperature for the (α+β)-annealing.

4.4. Fracture analysis

The first step taken to analyse the fracture of the samples was done with the macroscope. At first sight, the majority of the samples had a brittle behaviour at lower temperatures and while the testing temperature was risen, the frontiers between shear and brittle fracture surfaces started to be difficult to distinguish. In the (α+β)-annealing fractures, following the calculations of the proportion of shear fracture surface, the shear areas of the laterals of the sample start to diminish arising the temperature as shown in **Figure 7**. At 200ºC is still possible to identify some brittle fracture section, but at 400ºC it is not possible. At lower temperatures, the material was broken by the fracture toughness criteria, and at higher temperatures due to the reduction of the mechanical properties by the temperature, the material broke in a ductile way. In some samples tested at 400ºC, the sample did not fully break after the impact, so after the test the two halves of the samples were split up by hand.

In **Figure 7** it is shown different fracture surfaces at increasing temperatures of the (α+β)-annealing. The results of -25ºC and 24ºC where similar in the proportion of shear fracture surface so it is just shown the lowest temperature. It can be appreciated that in all the three fracture zones appear horizontal lines parallel to the V-notch and the crack propagation. At low temperatures, the roughness of the sample was almost flat, and when the testing temperature was increased, the flat surface of the fracture started to become curved in the end part of the cross-section. At 400ºC was more visible due to almost half of the fracture section had that curvature, and the parallel lines to the V-notch were wider than at lower temperatures. This could be associated to the increasing energy absorption capacity that the material has at higher temperatures allowing bigger higher plastic deformations.

On the other hand, the β-annealing did not show that kind of surface due to the microstructure and size of the grains. In **Figure 8** appears the fractured surfaces from lower to higher testing temperatures. It can be observed that there are not big differences on the morphology of the fractures at different temperatures. The only thing that is remarkable is that the deepness of the fracture surface increased when increasing the temperature of the test.

DOI: 10.13009/EUCASS2019-756

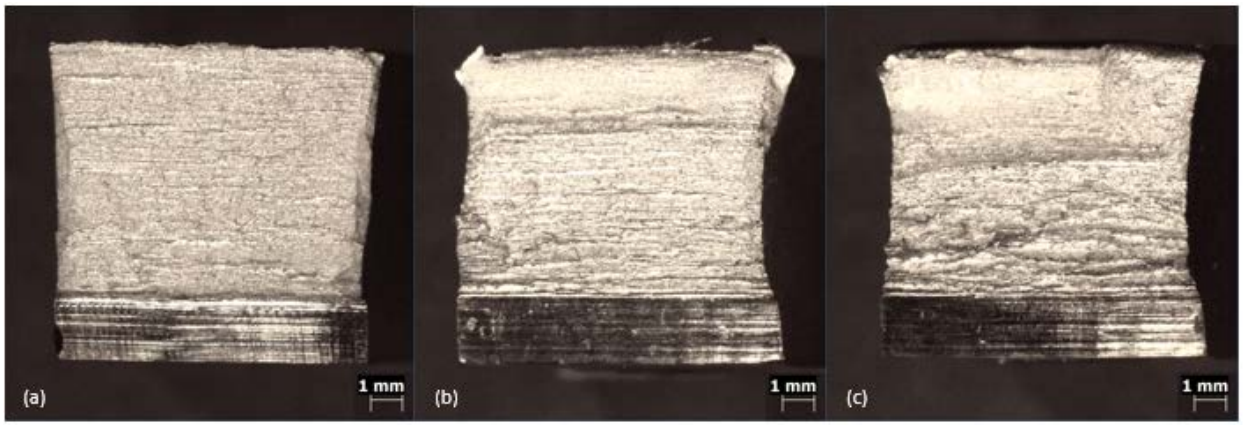

Figure 7. Fracture surfaces of (α+β)-annealing samples at (a)-25ºC, (b) 200ºC and (c) 400ºC.

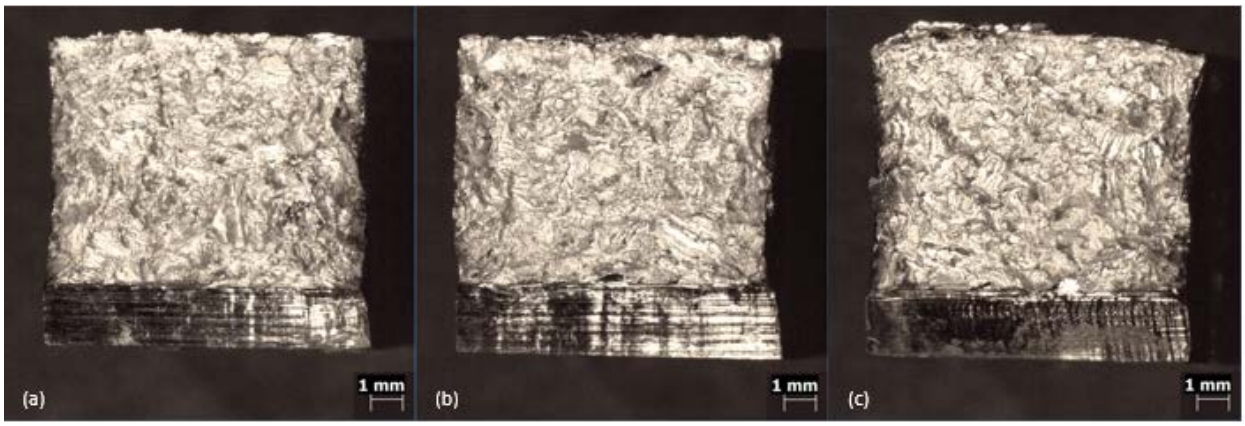

Figure 8. Fracture surfaces of β-annealing samples at (a)-25ºC, (b) 200ºC and (c) 400ºC.

From the micro-scale point of view, the most important fracture process observed was the nucleation, growth and coalescence of dimples, associated to a ductile fracture mechanism. In addition, some planar de-cohesion was observed in both microstructures.

The main fracture mechanism in the (α+β)-annealing was the dimple coalescence. Those dimples formed during the fracture process had different size along the crack propagation path. Near the V-notch the dimples were smaller than the dimples from the impacted face of the sample. This difference in size of the dimples can be explained by the sequence of the fracture process. At the beginning, the pendulous impact against the opposite face of the V-notch transmitting the energy to the sample. That energy crosses the cross-section of the sample and the fracture starts in the tip of the V-notch. Despite the impact toughness test is a dynamic test with a testing duration of less than a second, as the energy is being consumed to deform the material from the V-notch, the deformation process is lowering the plastic strain rate at the same time that the energy is being consumed. This has more influence in the high temperature tests due to the energy required to break the sample is bigger and it is close to the maximum energy that the pendulous can transfer to the sample.

Although most of the fracture process was ductile, there were some parallel bands to the V-notch with brittle behaviour. That horizontal lines can be associated to the history of the forging process as they are mostly α-phase and its fracture process is by planar de-cohesion. At higher temperatures, the appearance of this brittle lines were less prominent than at lower temperatures. A comparison of this phenomena is presented in **Figure 9**, where it can be observed that when the testing temperature arose, those brittle behaviour lines were diminishing and getting less significant. Relating the fracture microstructures with the fractured macrostructures, the parallel lines to the crack propagation direction in the macroscale can have some influence in the crack propagation process at the microscale as stated in [9].

DOI: 10.13009/EUCASS2019-756

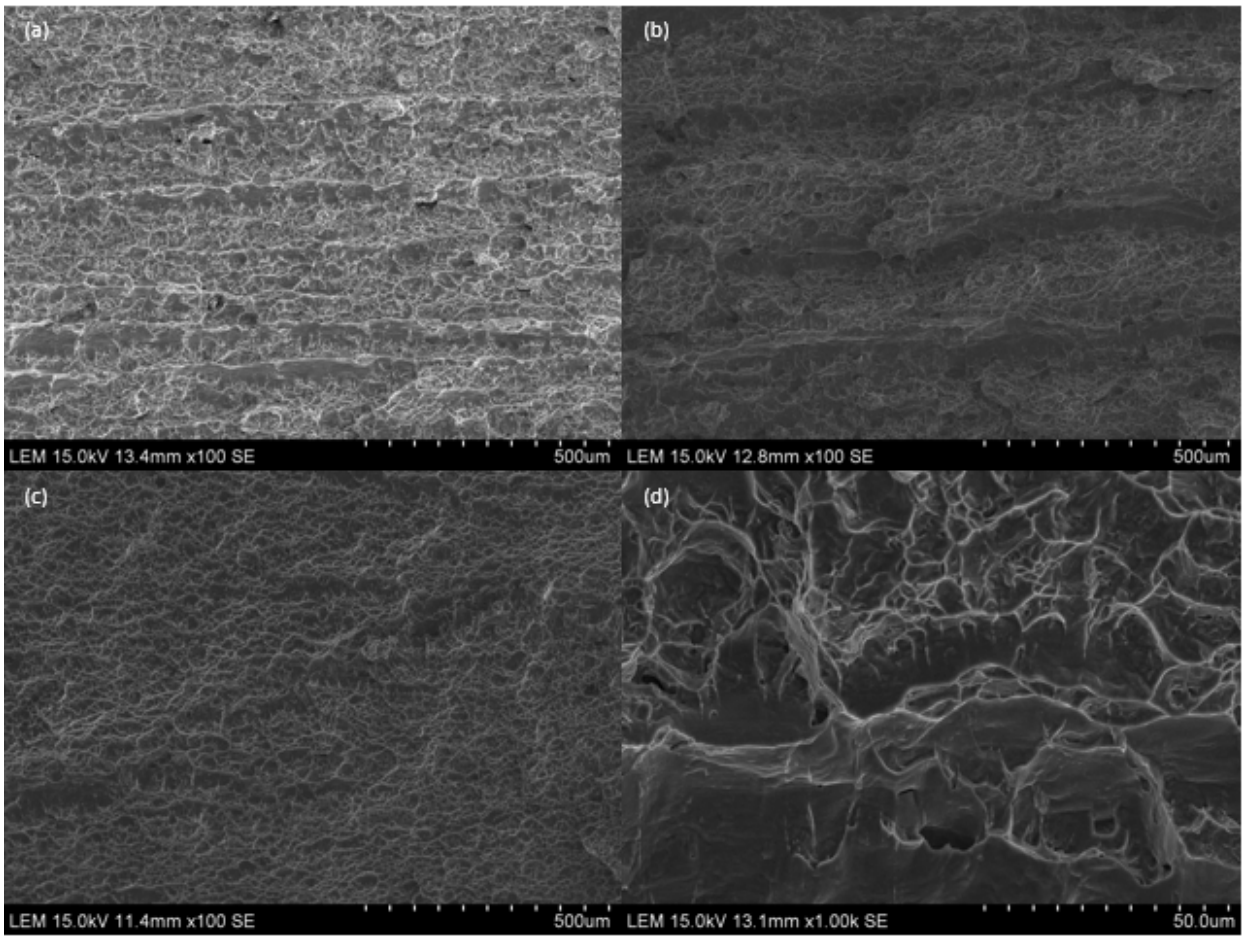

Figure 9. Fracture microstructures showing the mixture mode of dimples and brittle planar de-cohesion lines at (a)-25ºC, (b) 200ºC and (c) 400ºC. (d) Shows the detail of a border of that brittle behaviour lines.

The fracture behaviour of the β-annealing was slightly different from the commented mechanism of the (α+β)-annealing. In this case, due to the laminar microstructure of α-phase surrounded by β-phase forming the Widmanstätten structure, the fracture mechanisms were more brittle. With this microstructure, the majority of the plastic deformation is associated to the β-phase due to its body centred cubic lattice has more slipping systems for the moving of dislocations. The following micrographs exhibited in **Figure 10 (c) (d)** gives an example of this supposition. Comparing the morphology of the dimples from this heat treatment to the (α+β)-annealing, it can be observed that in this case the dimples are more plain and has less depth. This morphology is associated to the deployment of the β-phase that is placed between two α-platelets. When the plastic deformation is developed, the only system of deformation is in between those platelets, so it has a majority of planar shape.

The other part of the microstructure, the α-laminates has less slip systems than the β-phase and they tend to fracture by planar de-cohesion. Some examples of this fracture mechanism are shown in **Figure 10 (a) and (b)**, where it can be seen the shape of the α-platelets and some planar steps where de-cohesion has occurred. Another important fact compared with the (α+β)-annealing was that in this heat treatment there were no horizontal lines of brittle fracture due to the total recrystallization of the microstructure during the treatment.

DOI: 10.13009/EUCASS2019-756

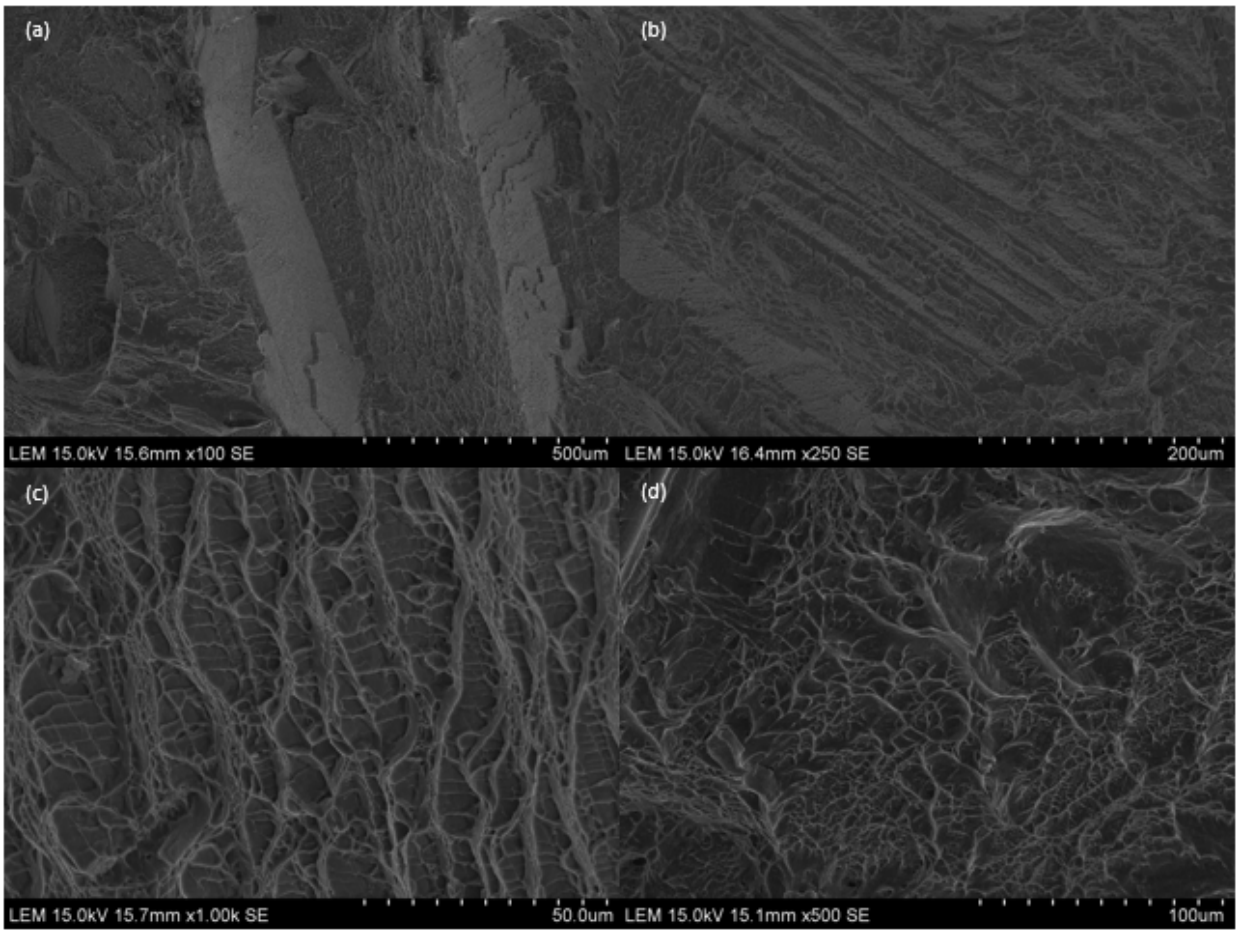

Figure 10. Images taken from β-annealing samples. (a) and (b) shows the de-cohesion planes with some roughness over the surface at -25ºC and (c) shows the ductile behaviour with shallow dimples in the same sample. (d) At 200ºC, an example of deformed β-phase over an α-platelet.

5. Conclusions

Despite the fact that more studies must be carried on testing different orientations of the material and different heat treatments to have a wider understanding of all the process, there are some preliminary conclusions that can be commented.

- Hexagonal closed packed lattices usually have a ductile to brittle transition temperature. In this case, at least at -25ºC that ductile to brittle transition temperature has not been observed. As titanium has the relationship of planar bases with the height smaller than the usual, this can affect to this behaviour and make the dislocation moving systems easier than in the standard hexagonal closed packed lattices.

- Laminar microstructures obtained from the β-annealing are less affected to the temperature changes than the (α+β)-annealing. This can be explained by the fully recrystallization of the samples while the heat treatment is being applied. As the microstructure had more time to develop, it is more stable against temperature variations.

- The fracture behaviour of the samples was totally influenced by the microstructure. Macroscopically, (α+β)-annealing had clearly differenced brittle plain part in the middle when plane strain conditions are obtained and shear fracture on the borders due to the loss of the plain strain condition. In addition, when increasing the testing temperature, shear fracture mode takes more importance and brittle fracture proportion is being reduced till almost most of the fracture surface is ductile. On the other hand, β-annealing behaviour was really different. For these samples, there were no differenced sections over the surface. The only appreciated

DOI: 10.13009/EUCASS2019-756

morphologies were high changes in the relief with no preferential orientation. When increasing the testing temperature, that relief was increased, but the general shape remained constant.

- Despite macroscopically the (α+β)-annealing fracture surfaces seemed to have brittle behaviour, when changing to the microscale, the majority of the fracture mechanisms were ductile. Most of the fracture surfaces were composed of dimples with increasing size from the V-notch to the impacted surface. An important thing observed was the parallel lines to V-notch with brittle behaviour, and when relating the micrographs with macrographs that lines can be identified in both images.

- The β-annealing fracture micromechanisms were slightly different. Beta phase have good plastic deformation thanks to its body centred cubic lattice, but the α-platelets do not have so much slip systems so they have more difficulties to deform. For this reason, a mixture mode of fracture was observed in this heat treatment. When propagating the crack, β-phase tended to plastic deform by dimples nucleation, growth and coalescence, but the α-platelets propagated the fracture by planar de-cohesion. As the microstructure is platelets of α-phase surrounded by β-phase, the fracture process was very influenced by the orientation of the platelets from the crack propagation plane.

Finally, as this is a preliminary work, it has been planned to study T-L, T-S and L-S orientations behaviour of these two heat treatments and in addition, test the four orientations of a solution treated and aged microstructure.

References

[1] Leyens C., Peters M. Titanium and Titanium alloys. Fundamentals and Applications. 2003. *Wiley-VCH*. ISBN 3-527-30534-3
[2] Ingaki I., Takechi T., Shirai Y.and Ariyasu N. 2014. Application and features of titanium for the aerospace industry. Nippon Steel & Sumitomo Metal Technical Report 106 July 2014.
[3] Lütjering G. Titanium. Engineering materials and processing. 2003. *Springer*. ISBN 3-540-42990-5
[4] ASTM E23 Standard Test Methods for Notched Bar Impact Testing of Metallic Materials. 200. *ASTM International*
[5] Muiriuri A.M., Maringa M., du Preez W.B.and Masu L.M. 2018. Variation of impact toughness of as-built DMLS Ti6Al4V (ELI) specimens with temperature. *South African Journal of Industrial Engineering* 29(3):284-298.
[6] Semenova I.P., Modina Ju., Polyakov A.V., Klevstov G.V., Klevtsova N.A., Pigaleva I.N. and Valiev R.Z. 2019. Charpy absorbed energy of ultrafine-grained Ti-6Al-4V alloy at cryogenic and elevated temperatures. *Materials Science & Engineering A*. 743:581-589,
[7] Wei Zhou, Chew K.G. 2003. Effect of welding on impact toughness of butt-joints in a titanium alloy. *Materials Science & Engineering A*. 347:180-185
[8] Boyer R., Welsch G., Collings E.W. Titanium alloys. Materials Properties Handbook.1994. *ASM International*. ISBN 0-871770-481-1.
[9] Buirette C. Huez J., Gey N. Vassel A., Andrieu E. 2014. Study of crack propagation mechanisms during Charpy impact toughness tests on both equiaxed and lamellar microstructures of Ti-6Al-4V titanium alloy. *Materials Science & Engineering A.* 618:546-557.